Nonlinear Analysis: Modelling and Control, 2008, Vol. 13, No. 2, 213–223

Conjugate Heat Transfer for a Vertical Flat Plate with Heat Generation Effect

A. A. Mamun[1], **Z. R. Chowdhury**[2], **M. A. Azim**[3], **M. A. Maleque**[4]

[1]Institute of Natural Sciences, United International University
Dhaka-1209, Bangladesh
mamun@uiu.ac.bd

[2]Department of Electrical and Electronic Engineering
United International University
Dhaka-1209, Bangladesh

[3]School of Business studies, Southeast University
Dhaka-1213, Bangladesh

[4]Department of Mathematics
Bangladesh University of Engineering and Technology
Dhaka-1000, Bangladesh

Received: 08.07.2007 **Revised:** 20.11.2007 **Published online:** 02.06.2008

Abstract. The heat generation effect on natural convection flow along and conduction inside a vertical flat plate is investigated. The developed governing equations with the associated boundary conditions for this analysis are transferred to dimensionless forms using a local non-similar transformation. The transformed non-linear equations of the non-dimensional equations are then solved using the implicit finite difference method with Keller box-scheme. Numerical results are found for different values of the heat generation parameter, conjugate conduction parameter and Prandtl number. The overall investigation of the velocity, temperature, skin friction and heat transfer rate are presented graphically.

Keywords: conjugate heat transfer, heat generation, vertical flat plate, finite difference.

Nomenclature

b	plate thickness	Nu_x	local Nusselt number
C_{fx}	local skin friction coefficient	p	conjugate conduction parameter
c_p	specific heat at constant pressure	Pr	Prandtl number
f	dimensionless stream function	Q	heat generation parameter
g	acceleration due to gravity	Q_0	constant
h	dimensionless temperature	q_w	heat flux
κ_f, κ_s	fluid and solid thermal conductivities, respectively	T_b	temperature at outside surface of the plate
l	length of the plate	T_f	temperature of the fluid

T_∞	fluid asymptotic temperature	η	dimensionless similarity variable
$\overline{u}, \overline{v}$	velocity components	τ_w	shearing stress
u, v	dimensionless velocity components	μ, ν	dynamic and kinematic viscosities, respectively
$\overline{x}, \overline{y}$	cartesian coordinates		
x, y	dimensionless cartesian coordinates	ρ	density of the fluid
β	coefficient of thermal expansion	ψ	stream function
θ	dimensionless temperature		

1 Introduction

The interaction between the conduction inside and the buoyancy forced flow of fluid along a solid surface is termed as conjugate heat transfer (CHT) process. In practical systems, such as heat exchangers, the convection in the surrounding fluid significantly influences the conduction in a tube wall. Accordingly, the conduction in the solid body and the convection in the fluid should be determined simultaneously.

The CHT problems have been studied by several research groups [1–3] with the help of mathematical models for simple heat exchanger geometries. Gdalevich et al. [4] and Miyamoto et al. [5] reviewed the early theoretical and experimental works of the CHT problems for a viscous fluid. Miyamoto observed that a mixed-problem study of the natural convection has to be performed for an accurate analysis of the thermo-fluid-dynamic (TFD) field if the convective heat transfer depends strongly on the thermal boundary conditions. Pozzi et al. [6] investigated the entire TFD field resulting from the coupling of natural convection along and conduction inside a heated flat plate by means of two expansions, regular series and asymptotic expansions. Moreover, Vynnycky et al. [7] studied the two dimensional conjugate free convection for a vertical plate of finite extent adjacent to a semi-infinite porous medium using finite difference techniques. Pop et al. [8] extended the analysis of Vynnycky for the mixed convection flow.

The CHT problems associated with the heat generating plate washed by laminar forced convection flow were studied by Karvinen [9], Sparrow et al. [10] and Garg et al. [11] using an approximate method. Moreover, an analytical and numerical solutions were performed by Vynnycky et al. [12] for the CHT problem associated with the forced convection flow over a conducting slab sited in an aligned uniform stream.

This article illustrates the effect of heat generation on the coupling of conduction inside and the laminar natural convection flow along a flat plate. According to the authors' best knowledge the effects have not been studied yet. The developed equations representing the effects are converted into the dimensionless equations by using suitable transformations with a goal to attain similarity solutions. The non-dimensional equations are then transformed into non-linear equations by introducing a non-similarity transformation. The resulting non-linear equations, together with their corresponding boundary conditions based on conduction and convection, are solved numerically with the help of the finite difference method utilizing Newton's linearization approximation. There are emphases on the evolution of the surface shear stress in terms of the local skin friction coefficient and the rate of heat transfer in terms of local Nusselt number. The velocity profiles as well as temperature distributions are also studied.

2 Mathematical analysis

A time independent natural convection flow of a viscous incompressible fluid along a vertical flat plate of length l and thickness b (Fig. 1) is considered.

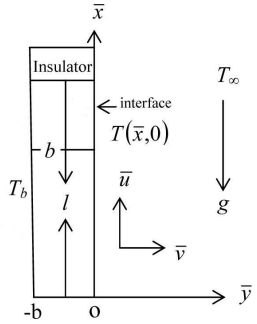

Fig. 1. Physical model and coordinate system.

A greater temperature T_b than the ambient temperature T_∞ is maintained constant at the outer surface of the plate. The governing equations of such flow under the usual boundary layer and the Boussinesq approximations can be written as

$$\frac{\partial \overline{u}}{\partial \overline{x}} + \frac{\partial \overline{v}}{\partial \overline{y}} = 0, \tag{1}$$

$$\overline{u}\frac{\partial \overline{u}}{\partial \overline{x}} + \overline{v}\frac{\partial \overline{v}}{\partial \overline{y}} = \nu\frac{\partial^2 \overline{u}}{\partial \overline{y}^2} + g\beta(T_f - T_\infty), \tag{2}$$

$$\overline{u}\frac{\partial T_f}{\partial \overline{x}} + \overline{v}\frac{\partial T_f}{\partial \overline{y}} = \frac{\kappa_f}{\rho\, c_p}\frac{\partial^2 T_f}{\partial \overline{y}^2} + \frac{Q_0}{\rho c_p}(T_f - T_\infty). \tag{3}$$

The term $\frac{Q_0}{\rho c_p}(T_f - T_\infty)$, Q_0 being a constant, represents the amount of generated or absorbed heat from per unit volume. Heat is generated or absorbed from the source term according as Q_0 is positive or negative.

The physical situation of the system suggests the following boundary conditions [13–16]

$$\left.\begin{aligned} &\overline{u} = 0,\ \ \overline{v} = 0, \\ &T_f = T(\overline{x}, 0),\ \ \frac{\partial T_f}{\partial \overline{y}} = \frac{\kappa_s}{b\kappa_f}(T_f - T_b) \end{aligned}\right\} \quad \text{on} \quad \overline{y} = 0,\ \ \overline{x} > 0,$$
$$\overline{u} \to 0,\ \ T_f \to T_\infty \quad \text{as} \quad \overline{y} \to \infty,\ \ \overline{x} > 0. \tag{4}$$

The governing equations and the boundary conditions (1)–(4) can be made dimensionless by using the following dimensionless quantities:

$$\begin{aligned} &x = \frac{\overline{x}}{l}, \quad y = \frac{\overline{y}}{l}Gr^{1/4}, \quad u = \frac{\overline{u}l}{\nu}Gr^{-1/2}, \quad v = \frac{\overline{v}l}{\nu}Gr^{-1/4}, \\ &\theta = \frac{T_f - T_\infty}{T_b - T_\infty}, \quad Gr = \frac{g\beta l^3\,(T_b - T_\infty)}{\nu^2} \end{aligned} \tag{5}$$

where Gr is the Grashof number and θ is the dimensionless temperature. The non-dimensional momentum and energy equations can now be written as

$$\frac{\partial u}{\partial x} + \frac{\partial v}{\partial y} = 0, \tag{6}$$

$$u\frac{\partial u}{\partial x} + v\frac{\partial u}{\partial y} = \frac{\partial^2 u}{\partial y^2} + \theta, \tag{7}$$

$$u\frac{\partial \theta}{\partial x} + v\frac{\partial \theta}{\partial y} = \frac{1}{Pr}\frac{\partial^2 \theta}{\partial y^2} + Q\theta \tag{8}$$

where $Q = \frac{Q_0 l^2}{\mu c_p Gr^{1/2}}$ is the heat generation parameter and $Pr = \frac{\mu c_p}{\kappa_f}$ is the Prandtl number. The corresponding boundary conditions in dimensionless forms are obtained as

$$\begin{aligned} &u = 0, \;\; v = 0, \;\; \theta - 1 = p\frac{\partial \theta}{\partial y} \quad \text{on} \;\; y = 0, \;\; x > 0, \\ &u \to 0, \;\; \theta \to 0 \quad \text{as} \;\; y \to \infty, \;\; x > 0 \end{aligned} \tag{9}$$

where $p = (\frac{\kappa_f b}{\kappa_s l})Gr^{1/4}$ is the conjugate conduction parameter. The present problem is governed by the magnitude of p as the heat generation parameter Q. This coupling parameter determines the significance of the conduction resistence within the wall.

The variables ψ, η and θ are considered in the following forms to solve the equation (7) and (8) for the boundary conditions described in (9):

$$\begin{aligned} \psi &= x^{4/5}(1+x)^{-1/20} f(x,\eta), \\ \eta &= y\, x^{-1/5}(1+x)^{-1/20}, \\ \theta &= x^{1/5}(1+x)^{-1/5}\, h(x,\eta), \end{aligned} \tag{10}$$

here η is a quasi-similarity variable and ψ is the non-dimensional stream function which satisfies the continuity equation related to the velocity components in the usual way as $u = \partial\psi/\partial y$ and $v = -\partial\psi/\partial x$. Moreover, $h(x,\eta)$ represents the dimensionless temperature. The dimensionless equations are obtained as:

$$f''' + \frac{16+15x}{20(1+x)} f f'' - \frac{6+5x}{10(1+x)} f'^2 + h = x\left(f'\frac{\partial f'}{\partial x} - f''\frac{\partial f}{\partial x}\right), \tag{11}$$

$$\begin{aligned} \frac{1}{Pr}h'' + \frac{16+15x}{20(1+x)} f h' - \frac{1}{5(1+x)} f' h + Q x^{2/5}(1+x)^{1/10} h \\ = x\left(f'\frac{\partial h}{\partial x} - h'\frac{\partial f}{\partial x}\right) \end{aligned} \tag{12}$$

where prime denotes partial differentiation with respect to η. The boundary conditions as mentioned in equation (9) then take the form:

$$\begin{aligned} &f(x,0) = f'(x,0) = 0, \\ &p\, h'(x,0) = -(1+x)^{1/4} + x^{1/5}(1+x)^{1/20} h(x,0), \\ &f'(x,\infty) \to 0, \quad h(x,\infty) \to 0. \end{aligned} \tag{13}$$

Equation (11) and (12) are solved numerically using the implicit finite difference method with Keller box scheme [17, 18] based on the boundary conditions as described in equation (13). The rate of heat transfer in terms of Nusselt number, Nu, and the shear stress in terms of the skin friction coefficient, C_f, are calculated because of their physical significance. These parameters can be written in the non-dimensional form as

$$C_f = \frac{Gr^{-3/4}l^2}{\mu\,\nu}\tau_w \quad \text{and} \quad Nu = \frac{lGr^{-1/4}}{\kappa_f(T_b - T_\infty)}q_w \tag{14}$$

where $\tau_w = \mu\,(\partial\overline{u}/\partial\overline{y})_{\overline{y}=0}$ and $q_w = -\kappa_f(\partial T_f/\partial\overline{y})_{\overline{y}=0}$ are the shearing stress and the heat flux, respectively. Using the new variables described in equation (5), equation (14) can be written as

$$C_{fx} = x^{2/5}(1+x)^{-3/20}f''(x,0), \tag{15}$$

$$Nu_x = -(1+x)^{-1/4}h'(x,0). \tag{16}$$

Besides, the numerical values of the surface temperature are also obtained from the relation

$$\theta(x,0) = x^{1/5}(1+x)^{-1/5}h(x,0). \tag{17}$$

We have also discussed the velocity profiles and the temperature distributions for different values of the heat generation coefficient, the conjugate conduction parameter and the Prandtl number.

3 Results

The main objective of the present work is to analyze the flow of the fluid and the heat transfer processes due to the conjugate heat transfer for a vertical flat plate. The Prandtl numbers are considered to be $4.24,\ 1.74,\ 1.0$ and 0.73 for the simulation that correspond to sulfur dioxide, water, steam and air, respectively. Detailed numerical results of the velocity, temperature, rate of heat transfer and skin friction coefficient for different values of the heat generation parameter, the conjugate conduction parameter and the Prandtl number are presented.

The temperature and the velocity fields obtained from the solutions of the equation (11) and (12) are depicted in Figs. 2–4. The increased value of the heat generation parameter means that more heat is produced and eventually, that heat increases the fluid motion as obtained in Figs. 2(a) and (b), respectively. The interfacial temperature, tabulated in Table 1, increases with the increasing Q at a particular position on the surface. Moreover, the solid-fluid interface temperature increases along the upward direction of the plate for a particular Q. Temperature variation at the interface for different Q is also observed due to the conduction within the wall.

The effect of the conjugate conduction parameter on the temperature and the velocity within the boundary layer with $Q = 0.01$ and $Pr = 0.73$ is shown in Figs. 3(a) and (b),

respectively. It can be noted from Fig. 3(a) that the temperature decreases monotonically with the increasing η for a particular value of p. The temperature and the velocity also decrease with the increasing p. A lower wall conductance κ_s or higher convective cooling effect due to greater κ_f and Gr increases the value of p as well as causes greater temperature difference between the two surfaces of the plate. The temperature at the solid-fluid interface is reduced since the temperature at the outside surface of the plate is kept constant. As a result the temperature profile as well as the velocity profile shifts downwards in the fluid. Numerical values, presented in Table 2, also show that the surface temperature decreases with the increased value of p for a particular value of Q and Pr. Moreover, the interfacial temperature along the upward direction of the plate increases for a particular value of p.

In Fig. 4, different values of Prandtl number with $Q = 0.01$, and $p = 1$ are considered for the velocity and temperature distributions. The peak velocity decreases as well as its position moves toward the interface with the increasing Pr. The overall temperature profiles also shift downwards with the increasing Pr as observed in Fig. 4(a). The physical fact that the thermal boundary layer thickness decreases with increasing Pr supports the result. The tabulated result in Table 3 also demonstrates that the surface temperature for a particular position decreases with the increasing Pr. Moreover, for a given Pr the surface temperature increases along the positive direction of x.

The variation of the local skin friction coefficient C_{fx} and local rate of heat transfer Nu_x with $Pr = 0.73$, and $p = 1.0$ for different values of Q at different positions are illustrated in Fig. 5(a) and (b), respectively. The heat generation accelerates the fluid flow, as mentioned earlier, and increases the shear stress at the wall. The increased skin friction coefficients with the increasing Q represent this phenomenon as illustrated in Fig. 5(a). Moreover, a hot fluid layer is created adjacent to the interface of the wall due to the heat generation mechanism and ultimately the resultant temperature of the fluid exceeds the surface temperature. Accordingly, the heat transfer rate from the surface decreases as shown in Fig. 5(b).

The variation of the reduced local skin friction coefficient C_{fx} and the local rate of heat transfer Nu_x for different values of p with x are shown in Fig. 6(a) and (b), respectively where $Q = 0.01$ and $Pr = 0.73$. The increased value of p decreases the velocity of the fluid within the boundary layer, as mentioned in Fig. 3(b), and decreases the viscosity of the fluid. As a result the corresponding skin friction coefficient decreases as shown in 6(a). On the other hand, from Fig. 6(b), it can be obseved that an increase in the p is associated with a decrease in the local rate of heat transfer. Fig. 7(a) and (b) deal with the effect of Pr on the skin friction coefficient and the rate of heat transfer against x with $Q = 0.01$ and $p = 1.0$. Fig. 7(a) shows that an increase in the Prandtl number Pr is associated with a decrease in the skin friction coefficient and from Fig. 7(b) it is seen that an increase in the Prandtl number Pr is associated with an increase in the rate of heat transfer.

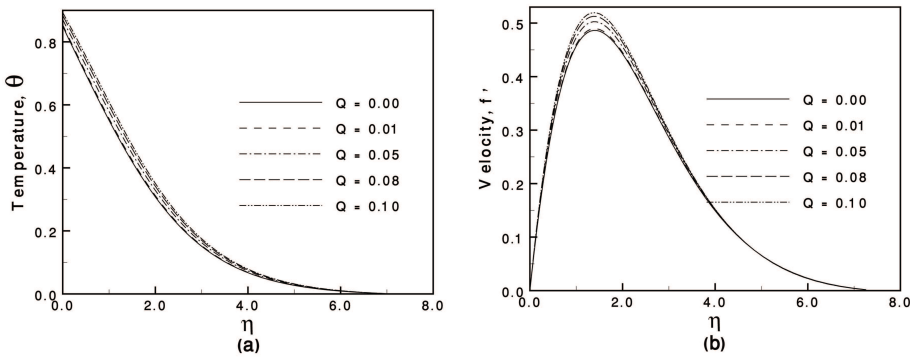

Fig. 2. (a) Variation of temperature profiles and (b) variation of velocity profiles against η for varying of Q with p = 1.0 and Pr = 0.73.

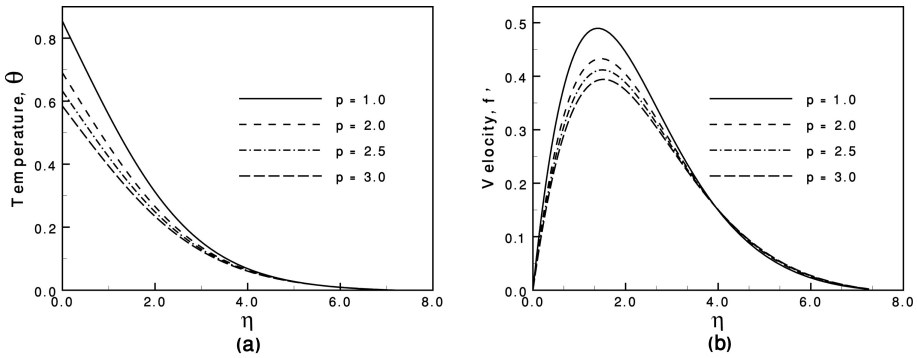

Fig. 3. (a) Variation of temperature profiles and (b) variation of velocity profiles against η for varying of p with Q = 0.01 and Pr = 0.73.

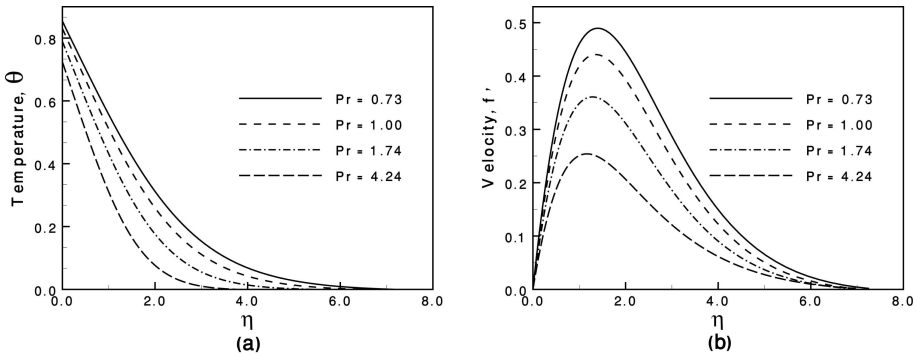

Fig. 4. (a) Variation of temperature profiles and (b) variation of velocity profiles against η for varying of Pr with Q = 0.01 and p = 1.0.

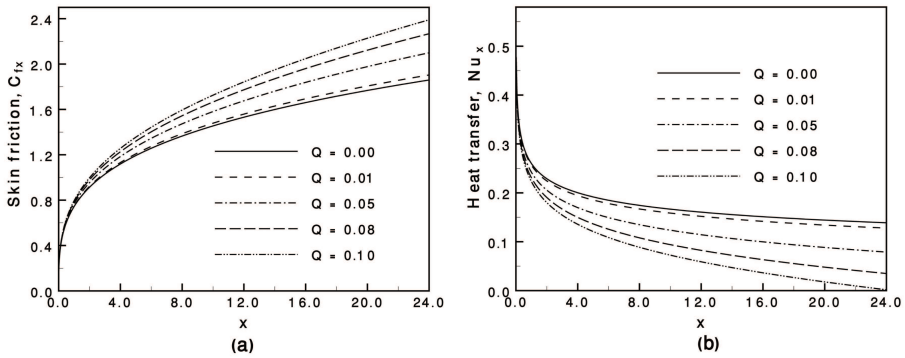

Fig. 5. (a) Variation of skin friction coefficients and (b) variation of rate of heat transfer against x for varying of Q with p = 1.0 and Pr = 0.73.

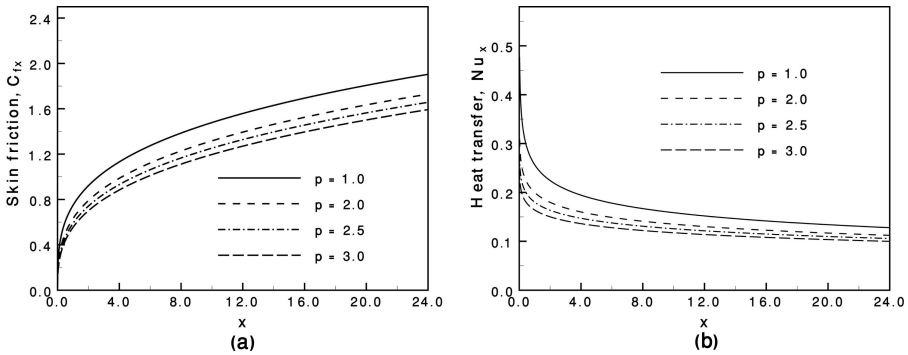

Fig. 6. (a) Variation of skin friction coefficients and (b) variation of rate of heat transfer against x for varying of p with Q = 0.01 and p = 1.0.

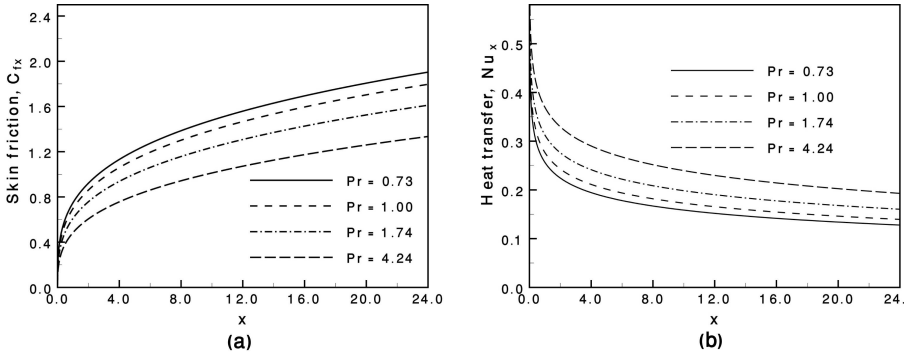

Fig. 7. (a) Variation of skin friction coefficients and (b) variation of rate of heat transfer against x for varying of Pr with Q = 0.01 and p = 1.0.

Table 1. Numerical values of surface temperature distribution against x for different values of Q when p = 1.0, Pr = 0.73

	$\theta(x,0)$			
x	(Q = 0.01)	(Q = 0.05)	(Q = 0.08)	(Q = 0.10)
0.0001	0.2604	0.2606	0.2608	0.2609
0.0801	0.6166	0.6215	0.6252	0.6277
0.1607	0.6533	0.6600	0.6651	0.6686
0.2423	0.6747	0.6827	0.6889	0.6930
0.3255	0.6898	0.6989	0.7059	0.7107
0.4108	0.7016	0.7116	0.7194	0.7246
0.4986	0.7113	0.7221	0.7306	0.7363
0.6605	0.7251	0.7373	0.7468	0.7533
0.7838	0.7334	0.7465	0.7566	0.7636
0.9981	0.7450	0.7593	0.7706	0.7783

Table 2. Numerical values of surface temperature distribution against x for different values of p when Q = 0.01, Pr = 0.73

	$\theta(x,0)$			
x	(p = 1.00)	(p = 2.00)	(p = 2.50)	(p = 3.00)
0.0001	0.2604	0.1529	0.1271	0.1087
0.0801	0.6166	0.4564	0.4073	0.3691
0.1607	0.6533	0.4951	0.4447	0.4049
0.2423	0.6747	0.5186	0.4677	0.4272
0.3255	0.6898	0.5356	0.4846	0.4436
0.4108	0.7016	0.5491	0.4980	0.4568
0.4986	0.7113	0.5604	0.5093	0.4679
0.6605	0.7251	0.5767	0.5257	0.4841
0.7838	0.7334	0.5867	0.5358	0.4942
0.9981	0.7450	0.6008	0.5501	0.5084

Table 3. Numerical values of surface temperature distribution against x for different values of Pr when Q = 0.01, p = 1.0

	$\theta(x,0)$			
x	(Pr = 0.73)	(Pr = 1.00)	(Pr = 1.74)	(Pr = 4.24)
0.0001	0.2604	0.2431	0.2157	0.1790
0.0801	0.6166	0.5905	0.5469	0.4829
0.1607	0.6533	0.6285	0.5863	0.5231
0.2423	0.6747	0.6507	0.6095	0.5471
0.3255	0.6898	0.6665	0.6261	0.5644
0.4108	0.7016	0.6788	0.6391	0.5781
0.4986	0.7113	0.6889	0.6499	0.5896
0.6605	0.7251	0.7034	0.6654	0.6061
0.7838	0.7334	0.7121	0.6747	0.6162
0.9981	0.7450	0.7242	0.6877	0.6303

4 Conclusion

A steady, two-dimensional, laminar natural convection flow is analyzed considering conduction and heat generation effects. The transformed partial differential equations together with the boundary conditions are solved numerically by implicit finite difference method. The effects of the heat generation parameter, conjugate-conduction parameter and Prandtl number are studied on the fluid flow and at the solid-fluid interface. The velocity of the fluid and the skin friction at the interface increase with the increasing heat generation parameter while they decrease with the increasing Prandtl number and conduction parameter. The temperature of the fluid increases with the increasing heat generation parameter and the decreasing conduction parameter and Prandtl number. Furthermore, the rate of heat transfer decreases with the increasing heat generation parameter, conduction parameter and the decreasing Prandtl number.

References

1. F. Meńdez, C. Treviño, The conjugate conduction-natural convection heat transfer along a thin vertical plate with non-uniform internal heat generation, *International Journal of Heat and Mass Transfer*, **43**, pp. 2739–2748, 2000.

2. O. Bautista, F. Meńdez, C. Treviño, Graetz problem for the conjugated-conduction film condensation process, *Journal of Thermophysics and Heat Transfer*, **14**, pp. 1–7, 2000.

3. C. Treviño, A. Espinoza, F. Meńdez, Steady state analysis of the conjugate heat transfer between forced counterflowing streams, *Journal of Thermophysics and Heat Transfer*, **10**, pp. 476–483, 1996.

4. L. B. Gdalevich, V. E. Fertman, Conjugate problems of natural convection, *Inzh.-Fiz. Zh.*, **33**, pp. 539–547, 1977.

5. M. Miyamoto, J. Sumikawa, T. Akiyoshi, T. Nakamura, Effects of axial heat conduction in a vertical flat plate on free convection heat transfer, *International Journal of Heat and Mass Transfer*, **23**, pp. 1545–1553, 1980.

6. A. Pozzi, M. Lupo, The coupling of conduction with laminar natural convection along a flat plate, *International Journal of Heat and Mass Transfer*, **31**, pp. 1807–1814, 1988.

7. M. Vynnycky, S. Kimura, Transient conjugate free convection due to a heated vertical plate, *International Journal of Heat and Mass Transfer*, **39**, pp. 1067–1080, 1996.

8. I. Pop, D. Lesnic, D. B. Ingham, Conjugate mixed convection on a vertical surface in a porous medium, *International Journal of Heat and Mass Transfer*, **38**, pp. 1517–1525, 1995.

9. R. Karvinen, Some new results for conjugate heat transfer in a flat plate, *International Journal of Heat and Mass Transfer*, **21**, pp. 1261–1264, 1978.

10. E. M. Sparrow, M. K. Chyu, Conjugated forced convection-conduction analysis of heat transfer in a plate fin, *International Journal of Heat and Mass Transfer*, **104**, pp. 204–206, 1982.

11. V. K. Garg, K. Velusamy, Heat transfer characteristics for a plate fin, *Journal of Heat Transfer*, **108**, pp. 224–226, 1986.

12. M. Vynnycky, S. Kimura, K. Kanev, I. Pop, Forced convection heat transfer from a flat plate: the conjugated problem, *International Journal of Heat and Mass Transfer*, **41**, pp. 45–59, 1998.

13. A. K. Luikov, Conjugate convective heat transfer problems, *International Journal of Heat and Mass Transfer*, **16**, pp. 257–265, 1974.

14. J. H. Merkin, I. Pop, Conjugate free convection on a vertical surface, *International Journal of Heat and Mass Transfer*, **39**, pp. 1527–1534, 1996.

15. I. Pop, D. B. Ingham, *Convective heat transfer*, Pergamon, Oxford, 2001.

16. C. L. Chang, Numerical simulation of micropolar fluid flow along a flat plate with wall conduction and buoyancy effects, *Journal of Applied Physics D*, **39**, pp. 1132–1140, 2006.

17. H. B. Keller, Numerical methods in the boundary layer theory, *Annual Reviews of Fluid Mechanics*, **10**, pp. 417–433, 1978.

18. T. Cebeci, P. Bradshaw, *Physical and computational aspects of convective heat transfer*, Springer, New York, 1984.